

Christopher W. MacIntosh\* and Matthew D. Parker  
North Carolina State University, Raleigh, NC

## 1. INTRODUCTION

Convective storms can either be considered surface-based or elevated depending on the source altitudes of their updraft parcels. Although the definition of convection that is considered elevated varies by author (e.g., Colman 1990a; Corfidi et al. 2008; Parker 2008; Nowotarski et al. 2011), a storm is generally determined to be elevated when it is situated over a statically stable layer that inhibits the lifting of inflow parcels from the near-surface (< ~500 m AGL) layer (Parker 2008; Nowotarski et al. 2011). Elevated convective environments may also contain near-zero surface-based convective available potential energy (CAPE) with appreciable instability present aloft (Colman 1990a,b; Grant 1995; Moore et al. 1998; Thompson et al. 2003; Horgan et al. 2007).

Elevated convection occurs over much of the United States, producing heavy rainfall, hail, and occasionally severe surface winds. Literature on elevated squall lines is prevalent (e.g., Bernardet and Cotton 1998; Bryan and Weisman 2006; Billings and Parker 2012); however, studies of elevated supercells are scarce (with the notable exception of Nowotarski et al. 2011). As a result, we have only a cursory understanding of processes associated with elevated supercells and the differences, if any, compared to surface-based supercells.

An operational challenge is that on Doppler radar, these storms look similar to surface-based cells; however, severe surface winds and tornadoes are rare in supercells over stable layers (e.g., Kis and Straka 2010). The current lack of knowledge about elevated supercells thus hinders forecasters, possibly resulting in higher false alarm rates for issued warnings.

During the second Verification of the Origins of Rotation in Tornadoes Experiment (VORTEX2), an unprecedented dataset showcasing an elevated supercell was obtained. This case from 6 May 2010 is the focus of this research, which aims to further the understanding of this subset of convective storms. Section 2 covers the methods

involved in the examination of the supercell. A case overview is presented in Section 3 with modeling results shown in Section 4. Preliminary conclusions and future work are exhibited in Section 5.

## 2. METHODS

### *a. Observations*

VORTEX2 employed an armada of mobile observational platforms in an effort to learn more about the dynamics of tornadoes and their parent supercells (Wurman et al. 2012); many of these instruments were utilized in this study. Soundings in the inflow of the supercell were launched using the GPS advanced upper-air sounding system (MGAUS). Two soundings in the near-inflow (~30-40 km from the updraft) and one in the far-inflow (~70-100 km from the updraft) were used in the analysis of this case (Fig. 1).

Surface kinematic and thermodynamic observations in the forward-flank, hook-echo and inflow area of the storm were made using mobile mesonets (Straka et al. 1996) and StickNets (Weiss and Schroeder 2008). Quality control and bias correction were performed on the data as well as a time-to-space conversion to help eliminate biases associated with mobile vs. stationary observations (Skinner et al. 2010).

Dual-Doppler analyses were completed for a handful of times using the Doppler On Wheels (DOW; Wurman et al. 1997, Wurman 2001) and Shared Mobile Atmospheric Research and Teaching (SMART-R; Biggerstaff et al. 2005) mobile radars. These involved using a two-pass Barnes filter (Barnes 1964) with a convergence parameter of 0.3 (Majcen et al. 2008). Data was translated using storm motion calculated from the Goodland, KS WSR-88D Doppler radar. The horizontal and vertical grid spacings were set to 250 m with a smoothing parameter of 0.85 km<sup>2</sup> and 1.6 km<sup>2</sup> in the horizontal and vertical for the DOWs and SMART-R, respectively, which were based on the suggestions of Pauley and Wu

---

\*Corresponding author address: Christopher W. MacIntosh, Department of Marine, Earth, & Atmospheric Sciences, North Carolina State University, Campus Box 8208, Raleigh, NC 27695-8208. Email: cwmacin2@ncsu.edu

(1990) and Trapp and Doswell (2000). Vertical velocity at the lower boundary was set to zero with the three-dimensional wind field integrated vertically upward using mass continuity. To prevent errors in the analysis, extrapolation was turned off.

### *b. Model simulation*

To work in tandem with the observational analysis, an idealized simulation of the elevated supercell was run using Cloud Model 1, version 16 (CM1; Bryan and Fritsch 2002). The model domain is 250 km x 250 km x 16 km with a horizontal grid spacing of 250 m. A stretched vertical grid (64 levels) ranging from 100 m in the lowest 3 km to 500 m above 9 km was used in an attempt to better resolve the stable layer near the surface. The model was started with a sounding representative of the observed environment, created by blending the two near-inflow soundings combined with the wind profile from the far-inflow sounding; the similarities between the hybrid model sounding and observed profiles are sufficient for use in the study (Figs. 1, 2). The moisture profile was reset to 95% relative humidity if necessary to prevent the presence of moist absolutely unstable layers. Convergence was initialized over the first 30 minutes of the simulation and maximized at the top of the stable layer to trigger convection; a warm bubble was not capable of producing a storm. The simulation was run out for four hours with a large time step of 2.0 s. Friction, Coriolis force, and radiational effects were neglected.

## **3. 6 MAY 2010 OBSERVATIONS**

During the day on 6 May 2010, a surface low was situated over southwestern Kansas with a somewhat diffuse quasi-stationary front draped eastward across the state. This forcing was the focus for convection as the target storm formed to the north of the front around 2243 UTC. This storm began to show supercellular characteristics over time as it approached the town of Oberlin, Kansas. VORTEX2 scientists presumed that this supercell was elevated due to the presence of cool, dry air near the surface and zero surface-based CAPE calculated from launched soundings. Radar reflectivity of the target storm shows the cell's steadiness over time, including a bow-like hook echo on the southern periphery (Fig. 3). This

suggests that some quasi-steady forcing must be present here, whether dynamic or perhaps in the form of waves or a strong cold pool.

Dual-Doppler analysis was possible at 0058 UTC 7 May 2010 using DOW6 and SMART-R2 (Fig. 4). In the lowest levels, i.e. below the inversion height, the wind field seems relatively undisturbed with a lack of vertical motion present, implying that the storm is indeed decoupled from the surface (as expected with elevated convection). Above the inversion height (~2 km), updraft/downdraft couplets begin to appear along with mesocyclonic curvature in the wind field. In many respects, the upper part of the storm resembles the classic appearance of a surface-based supercell.

To investigate the existence of wave-like activity associated with the stable layer, a north-south cross-section was taken through the hook echo (Fig. 5). As in Fig. 4, the flow beneath the inversion is steady and unperturbed by the storm; however, at and above the inversion, small wave-like perturbations start to appear in the vertical velocity field. This matches closely with the height where the updraft first starts to become evident in Fig. 4, suggesting that these waves could be playing a role in lifting parcels to their level of free convection (thereby maintaining the supercell's updraft). However, due to the lack of thermodynamic information in a dual-Doppler analysis, the type of wave (e.g., gravity waves) cannot be conclusively determined. Additionally, the origin and propagation characteristics of these waves have yet to be found and are the subject of future work.

Interestingly, the storm does not show signs of a downdraft-driven cold pool as is present in typical supercells, as evident from the absence of a  $\theta_e$  gradient at the surface (Fig. 6). A small cold pool (~2-3 K  $\theta$  deficit) does exist underneath the supercell, however, which is likely the result of evaporation of precipitation in the stable layer. Overall, the 6 May 2010 elevated supercell lacks many of the usual characteristics that are noted in classic surface-based supercells and may differ in terms of storm maintenance as well.

## **4. SIMULATION RESULTS**

Although unprecedented, the observations for this case are still limited in duration and scope. Therefore, an idealized model simulation was designed to advance our understanding. As in the

observations, the storm appears to be extremely steady over the span of the simulation (Fig. 7). The simulated storm is indeed a supercell with mesocyclone-scale values of vertical vorticity present at mid-levels (Fig. 8). The reflectivity below the inversion height (Fig. 9) also matches the observed storm structure (not shown) with the supercell having somewhat non-distinct characteristics in this layer. The reasons for this are currently under investigation, but may simply be due to the absence of a defined updraft/downdraft here.

The presence of waves has been documented in the simulation as well (Fig. 10). Ripples in the  $\theta$  surfaces combined with vertical velocity perturbations located behind the hook echo imply the existence of waves that may be assisting in maintaining the supercell updraft over time. As with the observations, the properties of these waves have not been determined at this point and are part of the future work plans.

A vital question is the origin of the updraft air in the simulated supercell. Although trajectories were not released in the current model simulation, five layers of passive tracer were set up to answer this. Fig. 11 shows a snapshot of the values of tracer at each level at one time. Clearly, very little air is drawn in from the stable layer, with the highest concentration of tracer appearing from the 1.5–2 km layer. Weak values of tracer do appear to be pulled into the updraft from the 0.5–1 km and 1–1.5 km layers. These layers have minimal (or no) CAPE, but may become involved through mixing and/or dynamic lifting. In terms of downdrafts, mid-level air fails to penetrate through the stable layer to the surface, reaching only 500 m with low concentrations (not shown).

## 5. CONCLUSIONS

The 6 May 2010 supercell from the VORTEX2 field project is perhaps the best-observed elevated supercell in history. Observations from instruments used in the field and an idealized model simulation helped to reveal some of intricacies of the storm as well as raise new questions. The following preliminary conclusions can be made about this case:

1. The supercell was certainly elevated and decoupled from the surface, evident from the undisturbed flow beneath the inversion and lack of updraft air originating in the

stable layer.

2. Wave-like disturbances on the inversion appear to assist in maintaining the supercell updraft over time.
3. Cooling from evaporation exists underneath the storm without evidence of mid-level downdrafts (i.e., “typical” outflow) reaching the surface.

The research is currently ongoing. In the future, a multi-Doppler, or an over-determined dual-Doppler, synthesis will be performed, likely using both DOWs and SMART-R2. This will provide a more complete analysis of the estimated observed winds, including better calculations of divergence and vertical vorticity.

Trajectories will be released in the model simulation to determine the origins of parcels in the updraft and downdraft of the supercell. Although the layers of passive tracer used in this study give a general idea of where the updraft air is coming from, trajectories are able to provide a relatively exact origin for each parcel. This will allow for useful calculations to be done, including determining the ratio of parcels that are pulled into the updraft from the stable layer. One of the key questions is whether the large horizontal vorticity present below the inversion is being tilted and advected into the storm by the updraft.

Additionally, the dynamics behind the maintenance and structure of the supercell are of great interest. Further information is needed regarding the role of the waves on the inversion. Are these waves actually the main forcing supporting the updraft throughout the storm’s life? Or is the upward-directed vertical perturbation pressure gradient force from the supercell itself more important? The bow-like appearance of the hook echo is another aspect that is being investigated. Sensitivity studies suggest that it may be related to strong lift along the edge of an elevated cold pool situated on the inversion.

Finally, the production of severe winds at the surface is another point that is greatly intriguing to the authors. This hazard was observed late in the lifetime of the 6 May 2010 storm, but was not replicated in the model simulation. Why are only a handful of elevated supercells able to produce severe winds at the surface? Future plans involve additional sensitivity studies and dynamical analyses.

*Acknowledgements.* The authors would like to thank Casey Davenport for her advice and helpful

notes on this case, the VORTEX2 PIs for making their datasets readily available, and members of the Convective Storms Group at NC State University for their feedback. This research is supported by the National Science Foundation under Grant AGS-1156123.

#### REFERENCES

- Barnes, S. L., 1964: A technique for maximizing details in numerical weather map analysis. *J. Appl. Meteor.*, **3**, 396–409.
- Bernardet, L. R., and W. R. Cotton, 1998: Multiscale evolution of a derecho-producing mesoscale convective system. *Mon. Wea. Rev.*, **126**, 2991–3015.
- Biggerstaff, M. I., and Coauthors, 2005: The Shared Mobile Atmospheric Research and Teaching radar: A collaboration to enhance research and teaching. *Bull. Amer. Meteor. Soc.*, **86**, 1263–1274.
- Billings, J. M., and M. D. Parker, 2012: Evolution and maintenance of the 22–23 June 2003 nocturnal convection during BAMEX. *Wea. Forecasting*, **27**, 279–300.
- Bryan, G. H., and J. M. Fritsch, 2002: A benchmark simulation for moist nonhydrostatic numerical models. *Mon. Wea. Rev.*, **130**, 2917–2928.
- , and M. L. Weisman, 2006: Mechanisms for the production of severe surface winds in a simulation of an elevated convective system. Preprints, *23rd Conf. on Severe Local Storms*, St. Louis, MO, Amer. Meteor. Soc.
- Colman, B. R., 1990a: Thunderstorms above frontal surfaces in environments without positive CAPE. Part I: A climatology. *Mon. Wea. Rev.*, **118**, 1103–1122.
- , 1990b: Thunderstorms above frontal surfaces in environments without positive CAPE. Part II: Organization and instability mechanisms. *Mon. Wea. Rev.*, **118**, 1123–1144.
- Corfidi, S. F., S. J. Corfidi, and D. M. Schultz, 2008: Elevated convection and castellanus: Ambiguities, significance, and questions. *Wea. Forecasting*, **23**, 1280–1303.
- Grant, B. N., 1995: Elevated cold-sector severe thunderstorms: A preliminary study. *Natl. Wea. Dig.*, **19** (4), 25–31.
- Horgan, K. L., D. M. Schultz, J. E. Hales, S. F. Corfidi, and R. H. Johns, 2007: A five-year climatology of elevated severe convective storms in the United States east of the Rocky Mountains. *Wea. Forecasting*, **22**, 1031–1044.
- Kis, A. K., and J. M. Straka, 2010: Nocturnal tornado climatology. *Wea. Forecasting*, **25**, 545–561.
- Majcen, M., P. M. Markowski, Y. Richardson, D. Dowell, and J. Wurman, 2008: Multipass objective analyses of Doppler radar data. *J. Atmos. Oceanic Technol.*, **25**, 1845–1858.
- Moore, J. T., A. C. Czarnetzki, and P. S. Market, 1998: Heavy precipitation associated with elevated thunderstorms formed in a convectively unstable layer aloft. *Meteor. Appl.*, **5**, 373–384.
- Nowotarski, C. J., P. M. Markowski, and Y. P. Richardson, 2011: The characteristics of numerically simulated supercell storms situated over statically stable boundary layers. *Mon. Wea. Rev.*, **139**, 3139–3162.
- Parker, M. D., 2008: Response of simulated squall lines to low-level cooling. *J. Atmos. Sci.*, **65**, 1323–1341.
- Pauley, P. M., and X. Wu, 1990: The theoretical, discrete, and actual response of the Barnes objective analysis scheme for one- and two-dimensional fields. *Mon. Wea. Rev.*, **118**, 1145–1163.
- Skinner, P. S., C. C. Weiss, Y. P. Richardson, and P. M. Marowski, 2010: Intercomparison between mobile and stationary surface observing platforms in VORTEX2. Preprints, *25th Conf. on Severe Local Storms*, Denver, CO, Amer. Meteor. Soc.
- Straka, J. M., E. N. Rasmussen, and S. E. Fredrickson, 1996: A mobile mesonet for finescale meteorological observations. *J. Atmos. Oceanic Technol.*, **13**, 921–936.
- Thompson, R. L., R. Edwards, J. A. Hart, K. L. Elmore, and P. Markowski, 2003: Close proximity soundings within supercell environments obtained from the Rapid Update Cycle. *Wea. Forecasting*, **18**, 1243–1261.
- Trapp, R. J., and C. A. Doswell III, 2000: Radar data objective analysis. *J. Atmos. Oceanic Technol.*, **17**, 105–120.
- Weiss, C. C., and J. L. Schroeder, 2008: StickNet: A new portable, rapidly-deployable surface observation system. *Bull. Amer. Meteor. Soc.*, **89**, 1502–1503.
- Wurman, J., J. Straka, E. Rasmussen, M. Randall, and A. Zahrai, 1997: Design and deployment of a portable, pencil-beam, pulsed, 3-cm Doppler radar. *J. Atmos. Oceanic Technol.*, **14**, 1502–1512.
- , 2001: The DOW mobile multiple-Doppler network. Preprints, *30th Int. Conf. on Radar Meteorology*, Munich, Germany, Amer. Meteor. Soc.
- , D. Dowell, Y. Richardson, P. Markowski, E. Rasmussen, D. Burgess, L. Wicker, and H. Bluestein, 2012: The Second Verification of the Origins of Rotation in Tornadoes Experiment: VORTEX2. *Bull. Amer. Meteor. Soc.*, **93**, 1147–1170.

Observed vs. Model Sounding, 6 May 2010

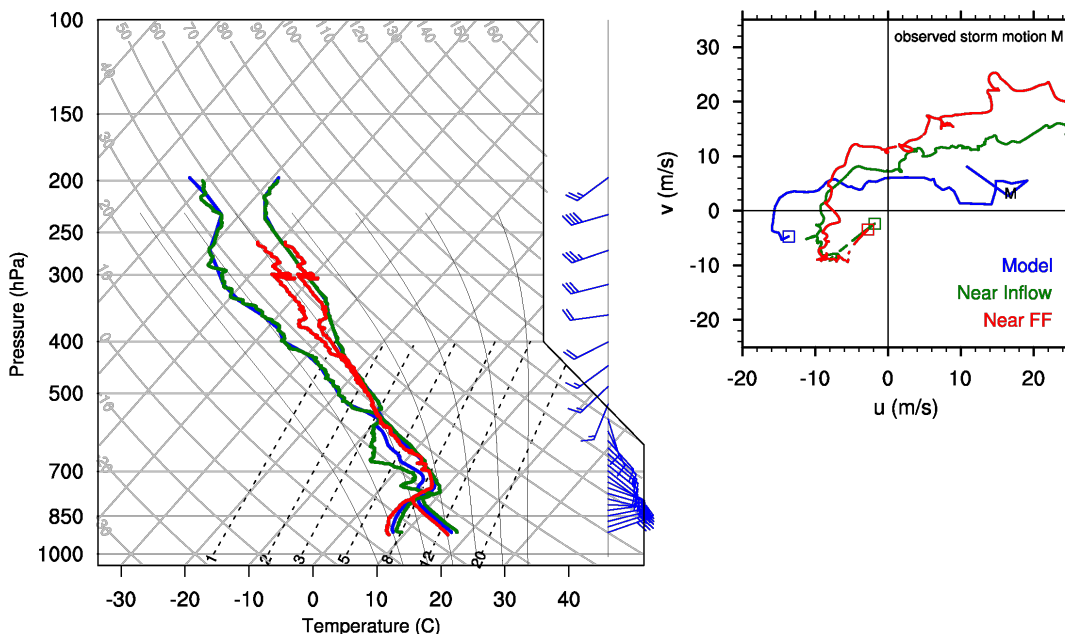


Figure 1: Soundings and hodographs from 6 May 2010 (green – near inflow taken at 0039 7 May 2010, red – near inflow taken at 0117 UTC 7 May 2010). Sounding used in the model simulation is shown in blue. Note that the wind profile on the sounding was used in the model and is from a far inflow sounding launched at 0106 UTC 7 May 2010.

Vertical Profiles of CAPE, CIN, LFC–parcel height, 6 May 2010

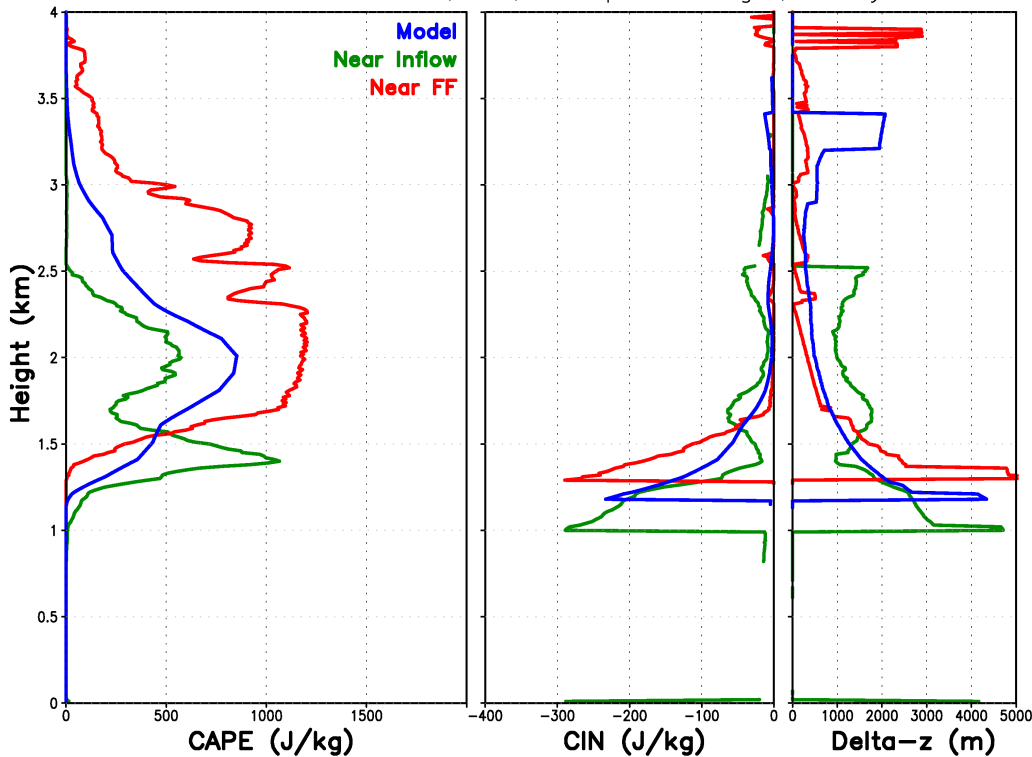


Figure 2: Vertical profiles of CAPE, CIN and delta-z (the distance between the parcel height and the level of free convection) for the soundings shown in Fig. 1.

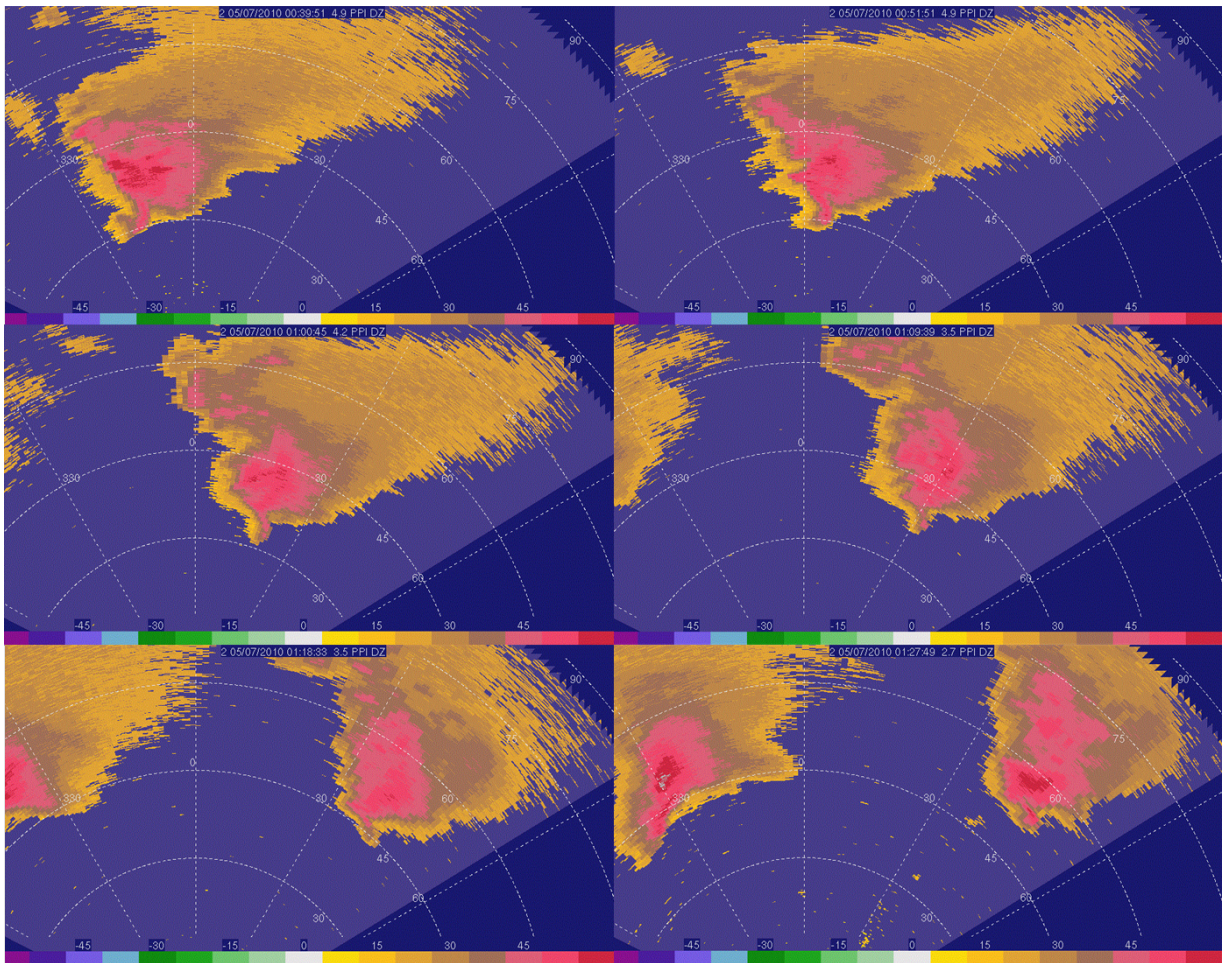


Figure 3: Plan view of reflectivity (dBZ) from the SMART-R2 mobile Doppler radar at (upper left to lower right) 0039, 0051, 0100, 0109, 0118, and 0127 UTC 7 May 2010. In each image, the height of the hook echo is ~2.5 km AGL.

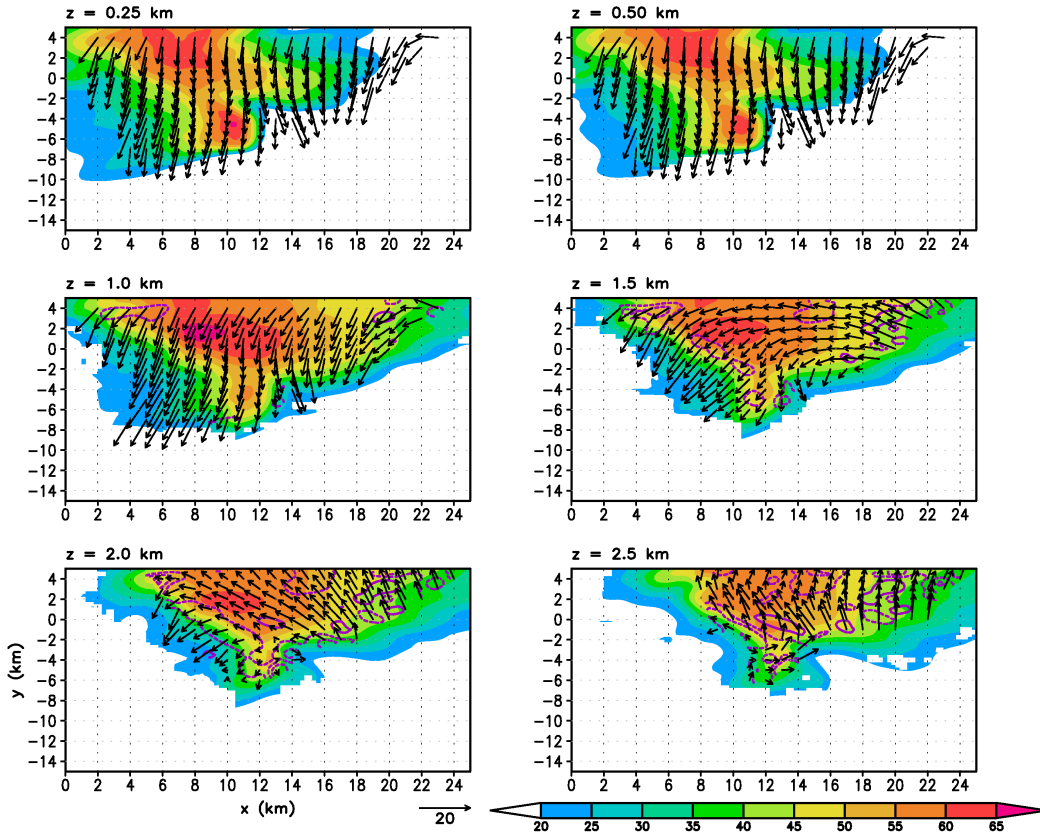


Figure 4: Plan view of analyzed reflectivity (shaded; dBZ), storm-relative wind vectors (m/s; derived from DOW6/SMART-R2 dual-Doppler synthesis) and vertical velocity (purple; contoured every 3 m/s, negative values dashed) at 0058 UTC 7 May 2010. Positions are relative to the location of DOW6 in km.

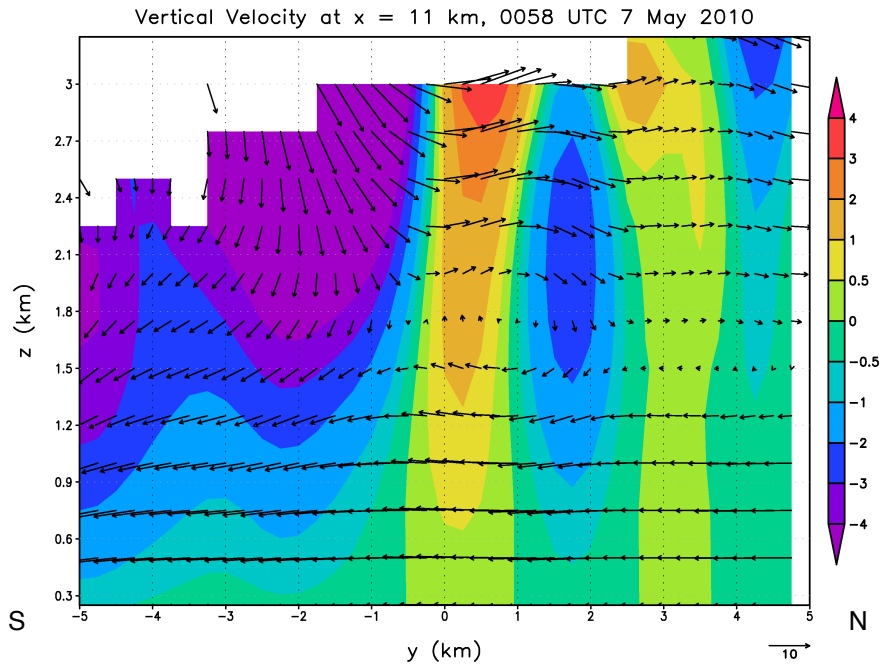


Figure 5: Vertical cross-section at  $x = 11$  km (see Fig. 4) of vertical velocity (shaded; m/s) and storm-relative wind vectors (derived from DOW6/SMART-R2 dual-Doppler synthesis) at 0058 UTC 7 May 2010.

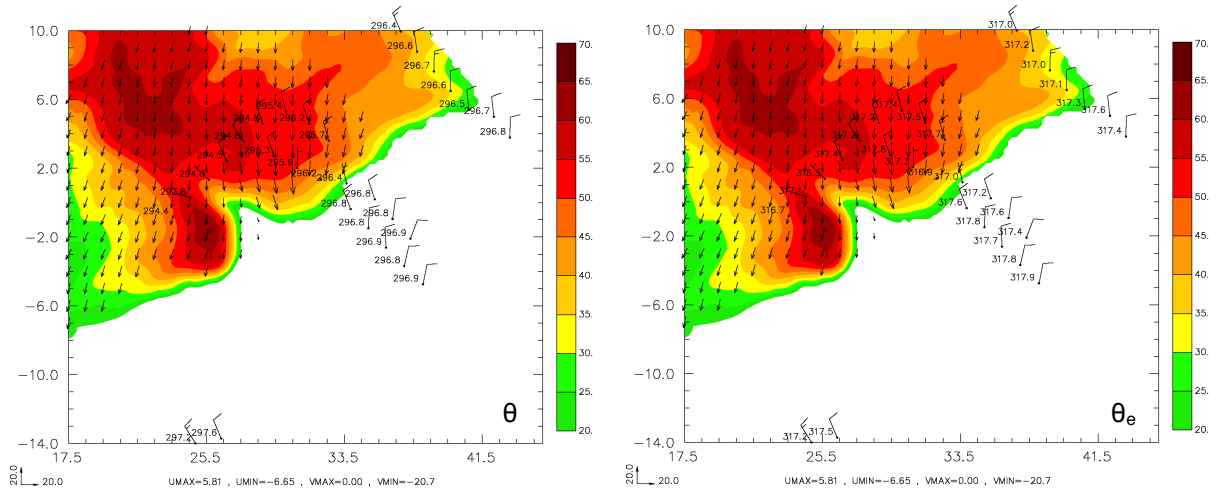


Figure 6: Plan view of analyzed reflectivity at 250 m AGL (shaded; dBZ), storm-relative wind vectors (250 m AGL; in m/s, derived from DOW6/DOW7 dual-Doppler synthesis) and time-to-space converted mobile mesonet and StickNet near-surface observations ( $\theta$  on left,  $\theta_e$  on right) at 0113 UTC 7 May 2010. Observation tracks are 3 minutes in length. Positions are relative to the location of DOW6 in km.

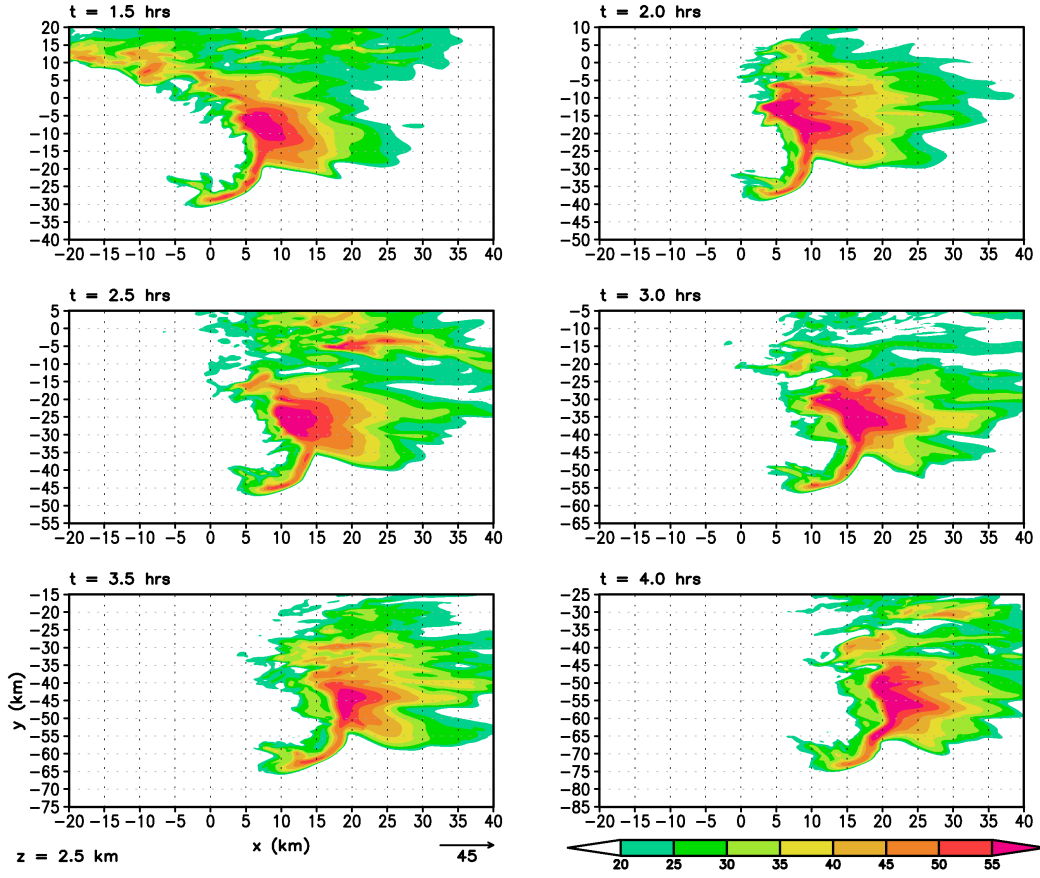


Figure 7: Plan view of simulated reflectivity (dBZ) at 2.5 km for various hours during the simulation. Box was moved to keep storm centered vertically.

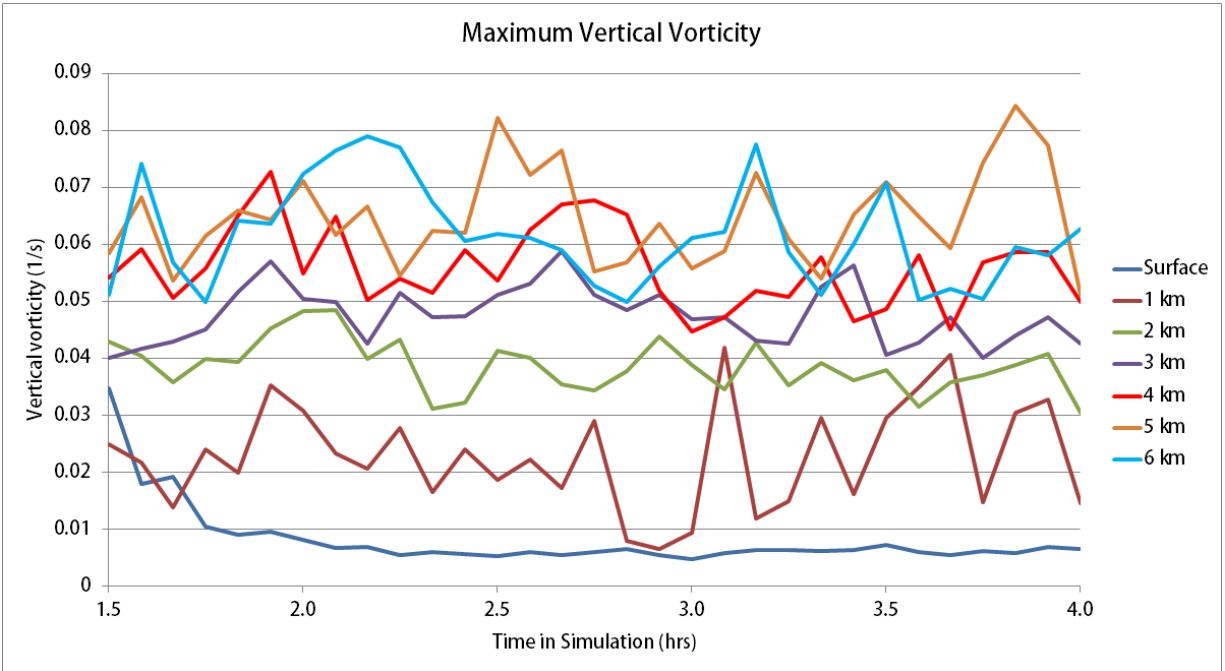


Figure 8: Maximum vertical vorticity ( $s^{-1}$ ) in the simulated supercell at various heights for a timespan of 1.5 to 4 hours in the simulation.

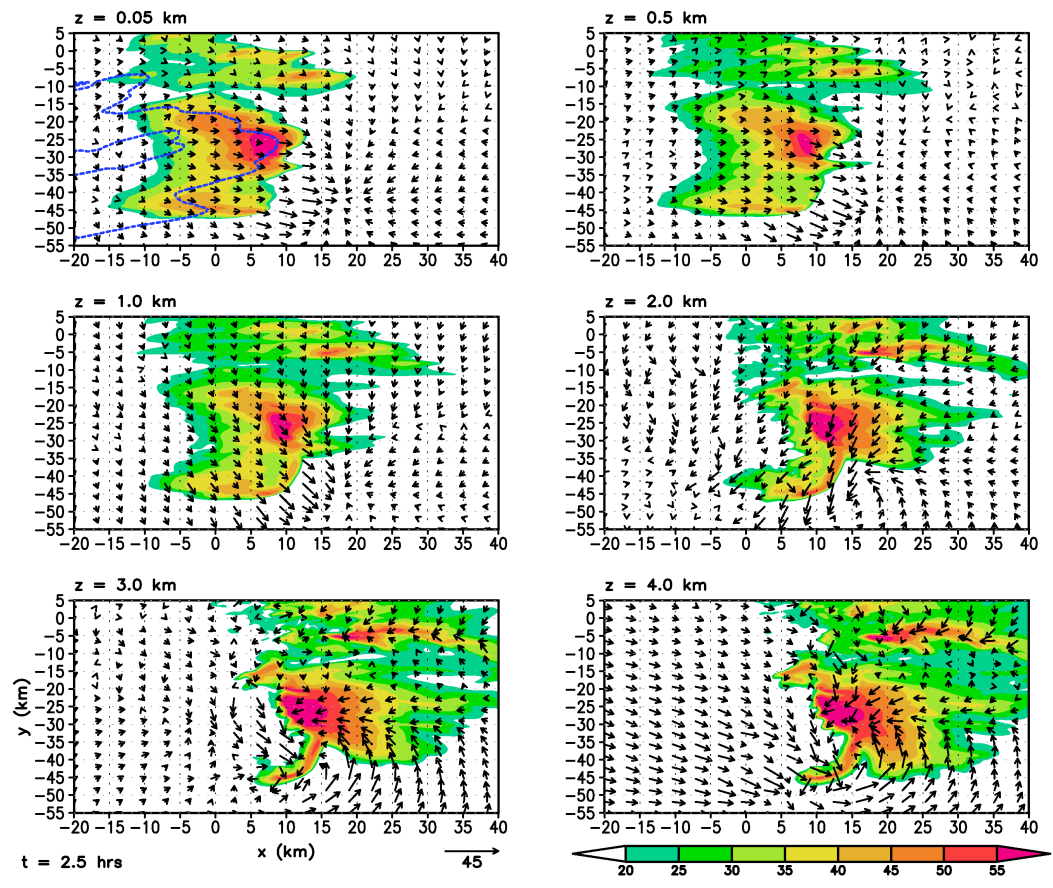


Figure 9: Plan view of simulated reflectivity (shaded; dBZ), perturbation wind vectors (m/s), and  $\theta$  deficit (blue; only shown at lowest model level, contoured at -1 and -3 K) at 2.5 hours into the simulation.

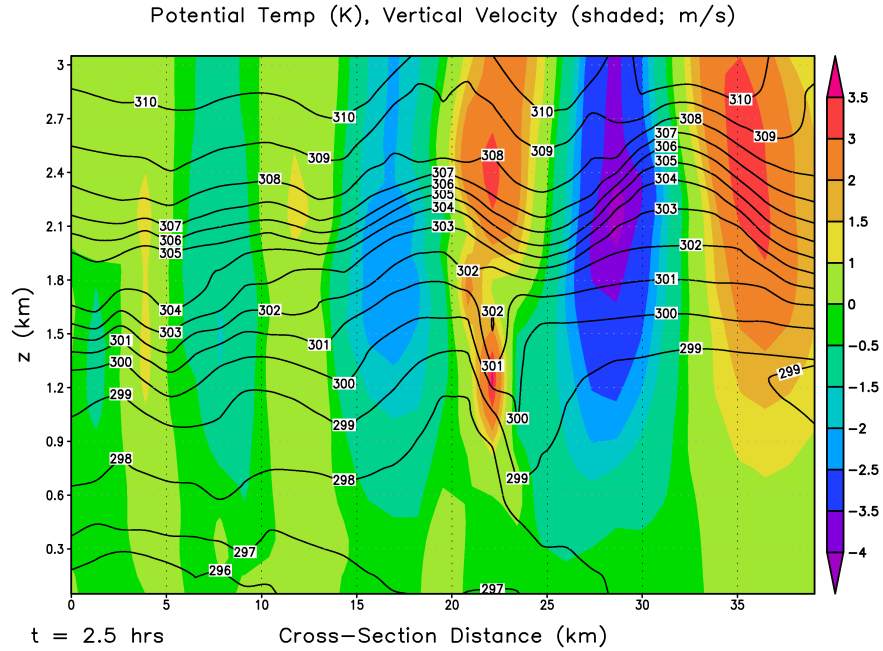


Figure 10: Vertical cross-section of  $\theta$  (contoured; K) and vertical velocity (shaded; m/s) from (-20, -30; left edge) to (10, -55; right edge) based on axes in Fig. 8 at 2.5 hours into the simulation.

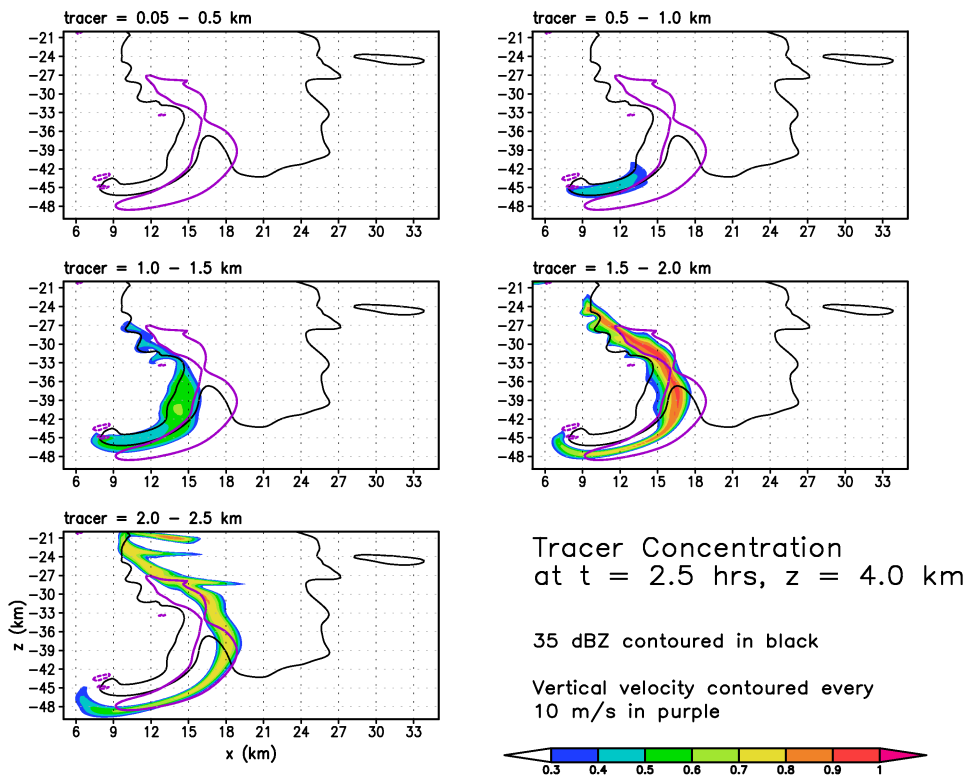


Figure 11: Plan view of concentration of a passive tracer (shaded), vertical velocity (purple; contoured every 10 m/s, negative values dashed), and the outline of the simulated supercell (black; 35 dBZ contour) at 4 km 2.5 hours into the simulation.